Macrocyclic Modification Using Organometallic Methodologies. Regiochemically Controlled Mono- and Bis-Homologation Reactions of Porphyrinogen with Carbon Monoxide Assisted by Early Transition Metals

Denis Jacoby,[†] Sylviane Isoz,[†] Carlo Floriani,*[,†] Angiola Chiesi-Villa,[‡] and Corrado Rizzoli[‡]

Contribution from the Institut de Chimie Minérale et Analytique, BCH, Université de Lausanne, CH-1015 Lausanne, Switzerland, and the Dipartimento di Chimica, Università di Parma, I-43100 Parma, Italy

Received October 7, 1994[⊗]

Abstract: The homologation of a pyrrole to a pyridine ring within the porphyrinogen skeleton was achieved with high selectivity, good yield, and controlled regiochemistry and was scaled up to multiple gram quantities. The homologation of *meso*-octaethylporphyrinogen to *meso*-octaethyltris(pyrrole)–monopyridine was carried out by reacting carbon monoxide with Zr–C and Zr–H functionalities supported by the *meso*-octaethylporphyrinogen ligand [$Et_8N_4H_4$]. The starting materials [(η^5-η^1-η^5-η^1-Et_8N_4)Zr(μ-NaH)]$_2$ (**2**) and [(η^5-η^1-η^5-η^1-Et_8N_4)Zr(μ-KH)]$_2$ (**3**) have been obtained by a direct addition of alkali hydrides to [(η^5-η^1-η^5-η^1-Et_8N_4)Zr(THF)] (**1**) or via hydrozirconation reactions in the cases of [{(η^5-η^1-η^1-η^1-Et_8N_4)ZrCH$_2$CH$_3$}$_2$(μ-K)$_2$] (**6**) and [{(η^5-η^1-η^1-η^1-Et_8N_4)ZrCH=CH$_2$}$_2$(μ-K)$_2$] (**7**). The reaction of **3** with carbon monoxide led to the intermediate formation of an η^2-formyl group possessing significant carbenium ion character, which was displayed in its addition to a pyrrole unit to give a pyridine ring in [{(η^5-η^1-η^5-η^1-Et_8-(C_4H_2N)$_3$$C_5H_3N$)Zr=O}$_2$($\mu$-K)$_2$] (**4**). The overall result is the formation of a novel macrocycle containing three pyrroles and one pyridine unit binding a zirconyl fragment derived from a complete cleavage of a C–O multiple bond. A straightforward hydrolysis of **4** with H_2O gave a high yield of the free macrocycle [Et_8(C_4H_2NH)$_3$(C_5H_3N)] (**5**). The carbonylation of **6** and **7** allowed the determination of the regiochemistry of the homologation reaction which gave, upon hydrolysis of the corresponding zirconyl complex, the following free macrocycles [Et_8(C_4H_2-NH)$_3$(3-RC_5H_2N)] [R = CH_2CH_3, **8**; R = CH=CH_2, **9**]. The intermediate η^2-acyl homologates one of the pyrroles to a *m*-alkylpyridine ring. By this methodology we are able to introduce functionalizable substituents into the pyridine ring, *i.e.*, in **9**. General procedures are reported for one-pot large-scale synthesis of free trispyrrole–monopyridine macrocycles. The reaction of [(η^5-η^1-η^1-η^1-Et_8N_4)Nb–Me] (**12**) with carbon monoxide led to the oxoniobium(V) complex [{η^5-η^1-η^1-η^1-Et_8(C_4H_2N)$_3$(*p*-MeC_5H_2N)}Nb=O] (**13**) due to the carbenium ion properties of the intermediate η^2-acetyl derivative. Complex **13** contains the *meso*-octaethyltrispyrrole–monopyridine trianion derived from the homologation of one of the pyrrole rings of [$Et_8N_4H_4$] into *p*-methylpyridine. The formation of a *para*-substituted pyridine is ascribed to the η^3 bonding mode of one of the pyrrolyl anions. The homologation of the trispyrrole–monopyridine macrocycle [Et_8(C_4H_2NH)$_3$(C_5H_3N)] (**7**) to the bispyrrole–bispyridine macrocycle has been achieved using a sequence which involves the key hafnium derivative [{η^5-η^1-η^5-η^1-Et_8(C_4H_2N)$_3$(C_5H_3N)}Hf–Me] (**17**). The reaction of **17** with carbon monoxide provides the homologation of a further pyrrolyl anion into *m*-methylpyridine, giving the *cis*-bispyridine–bispyrrole macrocycle binding the oxohafnium(IV) unit in [*cis*-Et_8(C_4H_2N)$_2$(C_5H_3N)(*m*-MeC_5H_2N)Hf=O] (**18**). The hydrolysis of **18** freed the ligand [Et_8(C_4H_2NH)$_2$(C_5H_3N)(*m*-MeC_5H_2N)] (**19**) which was characterized by an X-ray analysis. Crystallographic details: compound **8** is triclinic, space group $P\bar{1}$, a = 13.763(3) Å, b = 14.464(2) Å, c = 19.276(3) Å, α = 82.77(1)°, β = 89.71(2)°, γ = 76.52(1)°, Z = 2, and R = 0.045. Compound **13** is monoclinic, space group $C2/c$, a = 29.380(5) Å, b = 13.467(4) Å, c = 40.862(7) Å, α = γ = 90°, β = 107.55(2)°, Z = 16, and R = 0.047. Compound **17** is monoclinic, space group $P2_1/n$, a = 11.459(3) Å, b = 13.140(3) Å, c = 23.454(4) Å, α = γ = 90°, β = 102.23(3)°, Z = 4, and R = 0.026. Compound **19** is monoclinic, space group $P2_1/n$, a = 13.038(3) Å, b = 18.859(3) Å, c = 14.805(3) Å, α = γ = 90°, β = 102.80(2)°, Z = 4, and R = 0.057.

Introduction

A number of fundamental organometallic methodologies remain scientific curiosities without ever being of useful application to rather complex and interesting substrates or of being of use for synthetic purposes. In order to attain such a goal, the reaction should ideally be straightforward to apply, proceed in good overall yields, and be successful on a large scale.

This report deals with metal-assisted transformations of the porphyrinogen skeleton, **I**, the chemical and biochemical precursors of porphyrins,[1] to **II** to **III**. This conversion consists of the introduction of one carbon atom into up to two of the pyrrole rings, converting them into pyridine groups as depicted in Scheme 1. Such an homologation of pyrrole to pyridine leads

[†] Université de Lausanne.
[‡] Università di Parma.
[⊗] Abstract published in *Advance ACS Abstracts*, February 15, 1995.

(1) (a) *The Porphyrins*; Dolphin, D., Ed.; Academic: New York, 1978–1979; Vols 1–7. (b) Smith, K. M. *Porphyrins and Metalloporphyrins*; Elsevier: Amsterdam, 1975. (c) *Biosynthesis of Tetrapyrroles*; Jordan, P. M., Ed.; Elsevier: New York, 1991.

0002-7863/95/1517-2793$09.00/0 © 1995 American Chemical Society

Scheme 1

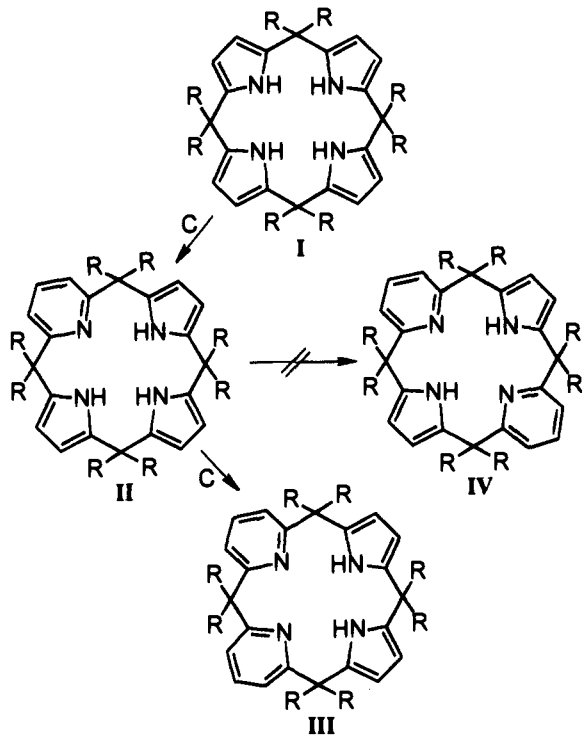

to otherwise hardly accessible tris(pyrrole)−monopyridine and bis(pyrrole)−bis(pyridine) macrocycles, related to porphyrinogen.

This modification has a large effect upon the electronic and topological characteristics of the macrocycle skeleton. Furthermore, we will show that the introduction of the carbon atom into the pyrrole ring can be obtained with a significant degree of regioselectivity.

The homologation of pyrrole to pyridine has been successfully achieved by exploiting some well-known organometallic reactions, for example the insertion of carbon monoxide into Zr−H and Zr−C bonds via the migration of the hydride and alkyl ligands.[2] This often-studied reaction produces carbenoid η^2-formyl and η^2-acyl groups.[2] The carbenoid form, when sterically protected toward dimerization (to yield an enediolato complex) or reduction, should react as such. In the present report we describe the addition of a carbenoid η^2-formyl or η^2-acyl to a pyrrole ring, followed by the complete cleavage of a C−O multiple[3] bond due to the presence of very oxophilic metal centers such as zirconium, hafnium, niobium, and potassium.

The *meso*-octaethylporphyrinogen[4] ligand exhibits some interesting characteristics which assist the transformations mentioned above. Specifically, the conformations derived from sp^3 carbons in the *meso* positions and the previously investigated porphyrinogen to zirconium bonding modes[5] create cavities,[6] assuring the stabilization of reactive intermediates at the metal and the geometrical proximity of reactive sites (pyrroles). The electron-rich periphery of porphyrinogen is further capable of binding an alkali cation,[7] and as will be seen, this property is of major assistance in the homologation reaction pathway.

The regiochemistry of the *meso*-octaethylporphyrinogen mono-homologation[8] leads either to the introduction of a *meta*-(zirconium and hafnium) or a *para*-substituted (niobium) pyridine ring depending on the nature of the metal. The metal also affects the bonding mode of the pyrrolyl units within the starting macrocyclic ligand which, in turn, directs the regiochemistry of further reactions. For example, the homologation of the tris(pyrrole)−monopyridine macrocycle **II** (Scheme 1), leading to the bis(pyrrole)−bis(pyridine) **III**, is possible using an appropriate sequence of organometallic reactions, but the choice of hafnium instead of zirconium is crucial. The preferential formation of the regioisomer **III** instead of **IV** is also controlled by the macrocycle bonding mode which is dictated by the metal. Assuming that only the η^5- or η^3-bonded pyrrole undergoes attack by a carbenoid fragment, the η^1-η^5 sequence in the bonding mode of the pyrrolyl anions within the macrocycle clarifies the observed regiochemistry. Preliminary results on the first step of the homologation reaction have been communicated.[7a]

Results and Discussion

In this report we will be concerned with chemistry derived from complex **1**, $[(\eta^5\text{-}\eta^1\text{-}\eta^5\text{-}\eta^1\text{-}Et_8N_4)Zr(THF)]$.[5a] A unusual property of **1** is its ability to behave as a bifunctional acid−base binding system for salts and ion-pair species, which as a consequence become soluble even in hydrocarbons.[5a] This is essentially due to the presence of an acidic site, *i.e.*, zirconium, and an electron-rich periphery supplied by the porphyrinogen skeleton. Complex **1** should therefore generally be viewed as a polar organometallic carrier. This is exemplified in the reaction of **1** with sodium or potassium hydride and in the formation of bimetallic zirconium−alkali metal hydrido derivatives **2**[5a] and **3**[7a] (Scheme 2), which have been recently reported.

It is the reaction of these metal hydride bridged dimers with carbon monoxide which paves the way for the pyrrole to pyridine transformation. The migratory insertion reactions of

(2) (a) Durfee, L. D.; Rothwell, I. P. *Chem. Rev.* **1988**, *88*, 1059. (b) Wolczanski, P. T.; Bercaw, J. E. *Acc. Chem. Res.* **1980**, *13*, 121. (c) Headford, C. E. L.; Roper, W. R. In *Reactions of Coordinated Ligands*; Braterman, P. S., Ed., Plenum: New York, 1986; Vol. 1, Chapter 8. (d) Carlin, D. J.; Lappert, M. F.; Raston, C. L. *Chemistry of Organo-Zirconium and -Hafnium Compounds*; Ellis Horwood: Chichester, U.K., 1986. (e) Labinger, J. A. *Transition Metal Hydrides*; Dedieu, A., Ed.; VCH: Weinheim, Germany, 1992.

(3) (a) Miller, R. L.; Wolczanski, P. T.; Rheingold, A. L. *J. Am. Chem. Soc.* **1993**, *115*, 10422 and references therein. (b) Chisholm, M. H.; Hammond, C. E.; Johnston, V. J.; Streib, W. E.; Huffman, J. C. *J. Am. Chem. Soc.* **1992**, *114*, 7056. (c) Bates, B. C. *Angew. Chem., Int. Ed. Engl.* **1993**, *32*, 228. (d) Neithamer, D. R.; LaPointe, R. E.; Wheeler, R. A.; Richeson, D. S.; Van Duyne, G. D.; Wolczanski, P. T. *J. Am. Chem. Soc.* **1989**, *111*, 9056. (e) Evans, W. J.; Grate, J. W.; Hughes, L. A.; Zhang, H.; Atwood, J. L. *J. Am. Chem. Soc.* **1985**, *107*, 3728 and references therein.

(4) (a) Fischer, H; Orth, H. *Die Chemie des Pyrrols;* Akademische Verlagsgesellschaft: Leipzig, 1934; p 20. (b) Dennstedt, M.; Zimmermann, J. *Chem. Ber.* **1887**, *20*, 850 and 2449; **1888**, *21*, 1478. (c) Dennstedt, D. *Chem. Ber.* **1890**, *23*, 1370. (d) Chelintzev, V. V.; Tronov, B. V. *J. Russ. Phys. Chem. Soc.* **1916**, *48*, 105, 127. (e) Sabalitschka, T.; Haase, H. *Arch. Pharm.* **1928**, *226*, 484. (f) Rothemund, P.; Gage, C. L. *J. Am. Chem. Soc.* **1955**, *77*, 3340.

(5) (a) Jacoby, D.; Floriani, C.; Chiesi-Villa, A.; Rizzoli, C. *J. Am. Chem. Soc.* **1993**, *115*, 3595. (b) Jacoby, D.; Floriani, C.; Chiesi-Villa, A.; Rizzoli, C. *J. Chem. Soc., Chem. Commun.* **1991**, 790. (c) Rosa, A.; Ricciardi, M.; Sgamellotti, A.; Floriani, C. *J. Chem. Soc., Dalton Trans.* **1993**, 3759.

(6) (a) Jacoby, D.; Floriani, C.; Chiesi-Villa, A.; Rizzoli, C. *J. Chem. Soc., Chem. Commun.* **1991**, 220. (b) Jubb, J.; Floriani, C.; Chiesi-Villa, A.; Rizzoli, C. *J. Am. Chem. Soc.* **1992**, *114*, 6571. (b) Piarulli, U.; Floriani, C.; Chiesi-Villa, A.; Rizzoli, C. *J. Chem. Soc., Chem. Commun.* **1994**, 895. (c) De Angelis, S.; Solari, E.; Floriani, C.; Chiesi-Villa, A.; Rizzoli, C. *J. Am. Chem. Soc.* **1994**, *116*, 5691 and 5702. (d) Solari, E.; Musso, F.; Floriani, C.; Chiesi-Villa, A.; Rizzoli, C. *J. Chem. Soc., Dalton Trans.* **1994**, 2015. (e) De Angelis, S.; Solari, E.; Floriani, C.; Chiesi-Villa, A.; Rizzoli, C. *J. Chem. Soc., Dalton Trans.* **1994**, 2467.

(7) (a) Jacoby, D.; Floriani, C.; Chiesi-Villa, A.; Rizzoli, C. *J. Am. Chem. Soc.* **1993**, *115*, 7025. (b) Jubb, J.; Jacoby, D.; Floriani, C.; Chiesi-Villa, A.; Rizzoli, C. *Inorg. Chem.* **1992**, *31*, 1306.

(8) For a general review on the homologation reaction of alcohols and related species, see: Chiusoli, G. P.; Salerno, G.; Foa, M. In *Reactions of Coordinated Ligands;* Braterman, P. S., Ed.; Plenum: New York, 1986; Vol. 1, Chapter 7. Parshall, G. W.; Ittel, S. D. *Homogeneous Catalysis*, 2nd ed.; Wiley: New York, 1992. Colquhoun, H. M.; Thompson, D. J.; Twigg, M. V. *Carbonylation*; Plenum: New York, 1991.

Scheme 2

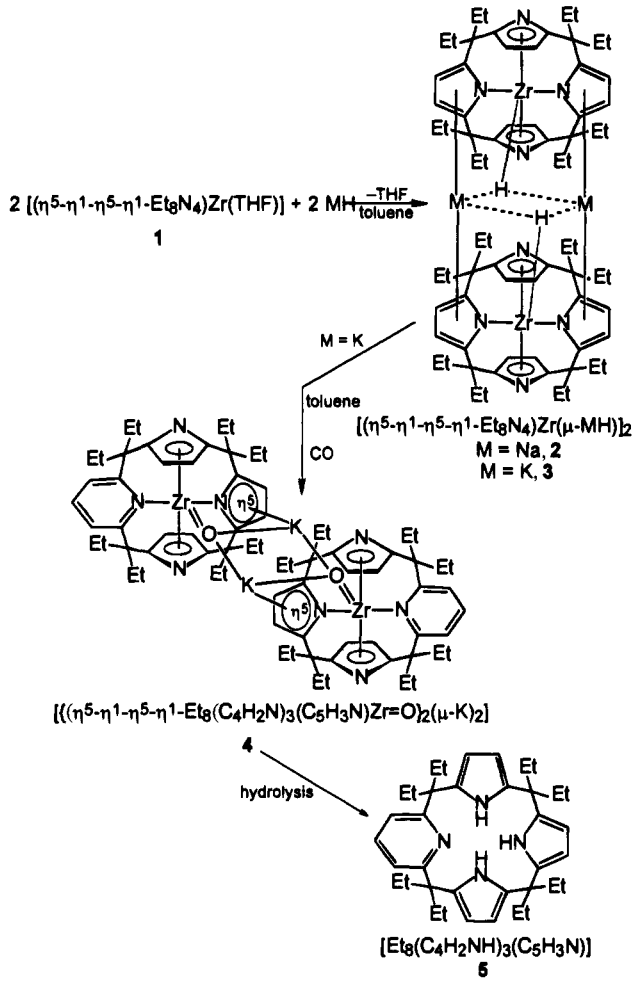

carbon monoxide with Zr−H (and Zr−C) bonds have mostly focused upon cyclopentadienyl and alkoxide-based systems.[2,3] The analogous reaction performed with **2** or **3** emphasizes the unusual roles porphyrinogen can play as an ancillary ligand. Indeed, the ability to bind alkali metal cations has already been alluded to. Further, the considerable three-dimensional bulk of the ligand provides the necessary steric protection for the organometallic functionality. Finally, the presence of reactive sites on the porphyrinogen itself should not be overlooked.

The reaction with carbon monoxide was initially carried out on the Zr−H bonds of complex **3** (Scheme 2). The absorption of carbon monoxide by **3** is a rather slow reaction requiring 2 days, but it nonetheless produces a white crystalline solid, **4**, in high yield (78%).

The structure of **4** shown in Scheme 2 is based on an X-ray analysis. The IR spectrum shows a very characteristic Zr=O band at 780 cm^{-1} [9] (the ^1H NMR spectrum is unremarkable). Details of the X-ray structure will be reported herein only for the analogous complex **8**.

The hydrolysis of **4** with H_2O under the mild conditions specified in the Experimental Section gave 90% of the free *meso*-octaethylmonopyridine−trispyrrole macrocycle **5**. The structure of **5** has been confirmed by all the analytical data, including an X-ray analysis, which will not be discussed since the analogous structure of the ethylpyridine-substituted macrocycle will be reported in detail. The major questions which arise at this stage are: (i) are the reactions in Scheme 2 an organometallic curiosity for producing small quantities of a ligand, which would otherwise be very difficult to produce, or is it a real synthetic method for producing significant amounts of macrocycle **5**? and (ii) can we explain the genesis of **4**?

Scheme 3

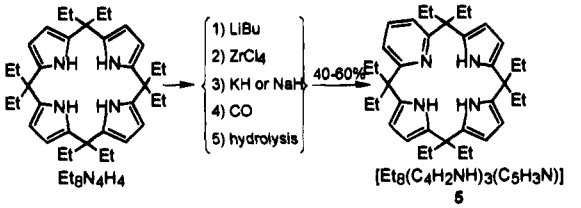

As far as the first question is concerned, we first tried to carry out all the steps separately leading to **5** on a large scale and then to perform Scheme 2 as a one-pot reaction. Both techniques were successful and we are now able to produce **5** with an overall yield of 40−60%, in quantities of up to 50 g. The entire sequence leading to **5** from $Et_8N_4H_4$ is summarized in Scheme 3 and reported in detail in the Experimental Section.

Even though we will not go into the details of all the various steps, the use of NaH instead of KH is essentially the same and the procedure is even simpler. We believe that the relevance of this synthetic methodology, which allows for a simple but significant modification of a rather large molecule, is extremely important. In the field of macrocyclic chemistry, the substituted forms of a macrocycle are currently obtained by a rather time consuming direct synthesis from the appropriate building blocks. This latter method is frequently poorly selective and often produces only small amounts of the desired molecule.[10]

Let us consider the genesis of **4**. The insertion of carbon monoxide into the Zr−H bond is a classic reaction in organometallic chemistry.[2] The reaction proceeds initially to the formation of a η^2-formyl species driven by the strong oxophilicity of the metal and then, in the absence of any steric protection, to a number of possible outcomes.[2]

The evolution of the η^2-formyl is essentially dictated by the nature and the steric characteristics of the ancillary ligand. In the present case the formyl functionality is formed in a cavity but, due to its carbenium ion nature,[2a,11] does not, however, stay as such and instead reacts with the unsaturated pyrrolyl anion. Then in the subsequent step an essential role is played by the presence of the alkali cation in enhancing the C−O multiple bond cleavage and in stabilizing the resultant oxo species.[3]

The pyrrole ring expansion to pyridine by a carbene source is a known, though poorly studied, reaction. Unlike our case, such examples proceed in a rather unselective manner and with poor yields.[12,13] The reaction could be mechanistically very different in the two cases, the electrophilic properties of the zirconium−η^2-formyl species being the major difference. Thus we can envisage in our case the electrophilic attack by the carbenium η^2-formyl to the pyrrole followed by the ring expansion. The preliminary step of this reaction is reminiscent

(9) Another zirconyl compound, [(η^5-C_5Me_5)$_2$ZrO(Py)] [ν(Zr=O), 780 cm^{-1}], has been very recently reported: Howard, W. A.; Waters, M.; Parkin, G. *J. Am. Chem. Soc.* **1993**, *115*, 4917.

(10) Lindoy, L. F. *The Chemistry of Macrocyclic Ligands*; Cambridge University Press: Cambridge, U.K., 1989. Dietrich, B.; Viout, P.; Lehn, J.-M. *Macrocyclic Chemistry*; VCH: Weinheim, Germany, 1993.

(11) Tatsumi, K.; Nakamura, A.; Hofmann, P.; Stauffert, P.; Hoffmann, R. *J. Am. Chem. Soc.* **1985**, *107*, 4440. Martin, B. D.; Matchett, S. A.; Norton, J. R.; Anderson, O. P. *J. Am. Chem. Soc.* **1985**, *107*, 7952. Roddick, D. M.; Bercaw, J. E. *Chem. Ber.* **1989**, *122*, 1579. Hofmann, P.; Stauffert, P.; Frede, M.; Tatsumi, K.; *Chem. Ber.* **1989**, *122*, 1559. Hofmann, P.; Stauffert, P.; Tatsumi, K.; Nakamura, A.; Hoffmann, R. *Organometallics* **1985**, *4*, 404. Tatsumi, K.; Nakamura, A.; Hofmann, P.; Hoffmann, R.; Moloy, K. G.; Marks, T. J. *J. Am. Chem. Soc.* **1986**, *108*, 4467.

(12) Jones, R. L.; Rees, C. W. *J. Chem. Soc. C* **1969**, 2249, 2255 and references therein. Fowler, F. W. *Angew. Chem., Int. Ed. Engl.* **1971**, *10*, 135.

Scheme 4

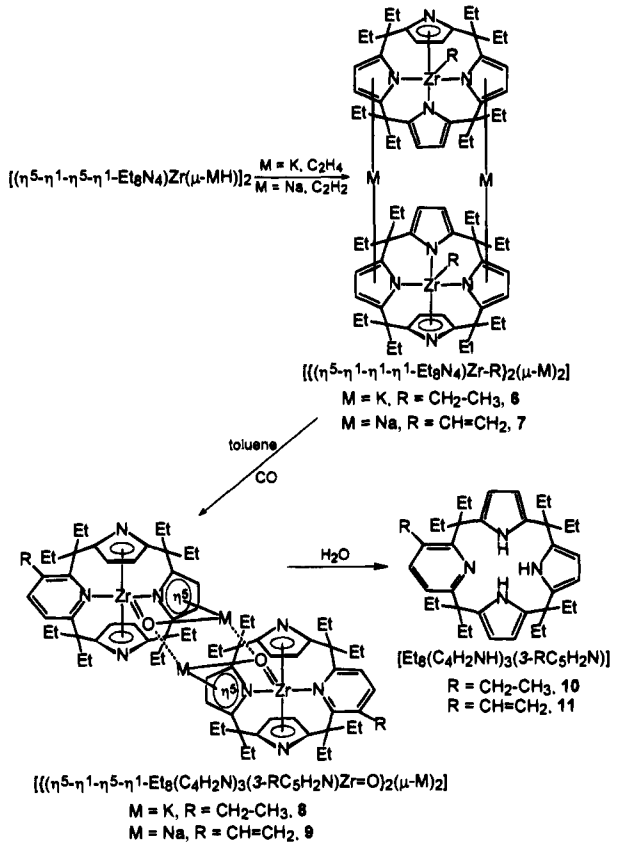

of the acylation of pyridine reported by Rothwell[14] as occurring via the intermediate formation of η^2-acyl functionalities, whose electrophilicity has been experimentally proved in the formation of pyridine adducts.[15]

The reactions involved in Scheme 2 emphasize the role of the oxophilic zirconium and potassium ions in enhancing the carbenium ion nature of the formyl functionality (*vide infra*). The stoichiometric result of the reaction is the homologation[8] of the pyrrole to pyridine by a "CH" unit as a consequence of a complete cleavage of the C−O bond. The oxygen from the CO molecule then forms a rare example of a terminal zirconyl unit. A single structurally documented example has been so far reported in the cyclopentadienyl chemistry, *i.e.*, $[(\eta^5\text{-}C_5Me_5)_2\text{-}Zr{=}O(Py)]$,[9] in addition to those we have prepared in the porphyrinogen−zirconium chemistry.[7a]

A major stereochemical consideration should be addressed in the pyrrole to pyridine conversion in Scheme 4, that is the regiochemistry of the homologation reaction. As the result of an attack by a carbenium ion on the pyrrole ring, the formyl carbon should be in the *meta* position of the final pyridine fragment. Such a regiochemistry is that observed in the ring expansion of pyrrole-pyridine when using carbenes.[12] In order to confirm such a regiochemistry, we studied the reaction of Zr−alkyl derivatives with carbon monoxide, as summarized in Scheme 4. The alkyl derivatives can be generated either via the hydrozirconation reaction[16] of the corresponding olefins or acetylenes or by a direct addition of lithium and potassium derivatives to **1**.[5a] The hydrozirconation of ethylene and acetylene occurs under relatively mild conditions and gives good yields of the corresponding ethyl and vinyl derivatives.[5a] The reaction of the dimers **6** and **7** with carbon monoxide in toluene led to **8** and **9**, which have been subsequentially hydrolyzed to **10** and **11**.

The reaction with carbon monoxide and the subsequent hydrolysis are both rather selective and lead to the corresponding product in good to excellent yield. The synthesis of **10** and **11** can be carried out almost as a one-pot reaction and does not require the isolation of the corresponding zirconyl intermediate **8** and **9**.

The analytical and spectroscopic characterization of **8**−**11** is reported in detail in the Experimental Section and does not show any striking difference from those of **4** and **5**. The data are fully consistent with the X-ray structure analysis we report here in detail for **8**. In the asymmetric unit of **8** there are two crystallographically independent $[\{\eta^5\text{-}\eta^1\text{-}\eta^5\text{-}\eta^1\text{-}Et_8(C_4H_2N)_3(3\text{-}EtC_5H_2N)\}Zr{=}O]$ anions [labeled A (Figure 1A) and B], linked as dimers by two potassium cations (Figure 1B). The two independent molecules have similar geometries. Hereafter the values referring to molecule B will be given in square brackets. The trispyrrole fragment is η^5,η^1,η^5-bonded to zirconium, while the substituted pyridine fragment interacts with the metal at a much longer distance of 2.525(4) [2.551(5)] Å (Table 2). The geometry of the whole molecule is very close to that observed in the analogous derivative containing a pyridine fragment instead of an Et-pyridine fragment.[7a] The four nitrogen atoms lie on a plane from which zirconium is displaced by only 0.089(1) [0.067(1)] Å in a direction opposite to the oxygen atom. The saddle shape conformation of the anion is close to that observed in **1**. The two η^5-pyrrole rings are bent to accommodate the σ-bonded N1,N3,O1 in a geometry approaching that of a $[Cp_2Zr]$ fragment. The zirconium atom lies in the plane defined by the σ-bonded atoms which is perpendicular to that containing zirconium and the centroids of the η^5-bonded rings (dihedral angles 89.1(1) [89.0(2)] Å). As we observed in **1** the coordination of the oxygen atom from THF causes a widening of the N1−Zr−N3 angle (175.7(2) [177.8(2)]°), so that the overall coordination geometry can be described as a *pseudo* trigonal bipyramid with N1 and N3 occupying the axial positions (Table 2). The Zr−O distances (1.802(5) [1.806(6)] Å) are very short, as expected for a double bond, and are in close agreement with the value observed in unsubstituted pyridine derivative [1.813(2) Å] and in $[(\eta^5\text{-}C_5Me_5)_2Zr(Py)O]$ [1.804(4) Å].[9] The K1A and K1B potassium cations display a strong η^5-interaction with the Zr-η^1-bonded pyrrolyl anions (Figure 1B and Table

(13) An interesting analogy can be found in the conversion of cyclopentadienyl anion into an alkylbenzene during the carbonylation of $[(\eta^5\text{-}C_5H_5)_3UR]$: Villiers, C.; Adam, R.; Ephritikhine, M. *J. Chem. Soc., Chem. Commun.* **1992**, 1555. Related transformations can be found in: De Boer, E. J. M.; De With, J. J. *Organomet. Chem.* **1987**, *320*, 289. Hessen, B.; Blenkers, J.; Teuben, J. H.; Helgesson, G.; Jagner, J. *Organometallics* **1989**, *8*, 2809. Meyer, T. Y.; Messerle, L. *J. Am. Chem. Soc.* **1990**, *112*, 4564.

(14) Fanwick, P. E.; Kobriger, L. M.; McMullen, A. K.; Rothwell, I. P. *J. Am. Chem. Soc.* **1986**, *108*, 8095.

(15) Arnold, J.; Tilley, T. D.; Rheingold, A. L. *J. Am. Chem. Soc.* **1986**, *108*, 5355.

(16) Schwartz, J.; Labinger, J. A. *Angew. Chem., Int. Ed. Engl.* **1976**, *15*, 333. Carr, D. B.; Yoshifuji, M.; Shoer, L. I.; Gell, K. I.; Schwartz, J. *Ann. N.Y. Acad. Sci.* **1977**, *295*, 127. Hart, D. W.; Blackburn, T. F.; Schwartz, J. *J. Am. Chem. Soc.* **1975**, *97*, 679. Hart, D. W.; Schwartz, J. *J. Am. Chem. Soc.* **1974**, *96*, 8115. Gibson, T. *Tetrahedron Lett.* **1982**, *23*, 157. Bock, P. L.; Boschetto, D. J.; Rasmussen, J. R.; Demers, J. P.; Whitesides, G. M. *J. Am. Chem. Soc.* **1974**, *96*, 2814. Labinger, J. A.; Hart, D. W.; Seibert, W. E.; Schwartz, J. *J. Am. Chem. Soc.* **1975**, *97*, 3851. Bertelo, C. A.; Schwartz, J. *J. Am. Chem. Soc.* **1976**, *98*, 262; **1975**, *97*, 228. Blackburn, T. F.; Labinger, J. A.; Schwartz, J. *Tetrahedron Lett.* **1975**, *16*, 3041. Neghishi, E.; Yoshida, T. *Tetrahedron Lett.* **1980**, *21*, 1501. Neghishi, E.; Takahashi, T. *Aldrichimica Acta* **1985**, *18*, 31. Neghishi, E.; Miller, J. A.; Yoshida, T. *Tetrahedron Lett.* **1984**, *25*, 3407. Jordan, R. F.; Lapointe, R. E.; Bradley, P. K.; Baenzinger, N. *Organometallics* **1989**, *8*, 2892 and references therein. For a survey of group IV and V hydrides, see: Toogood, G. E.; Wallbridge, M. G. H. *Adv. Inorg. Chem. Radiochem.* **1982**, *25*, 267. Cardin, D. J.; Lappert, M. F.; Raston, C. L. In *Comprehensive Organometallic Chemistry*; Wilkinson, G., Stone, F. G. A., Abel, E. W., Eds.; Pergamon: Oxford, 1981; Vol. 3, Chapter 23.2, p 45. Schwartz, J. *Pure Appl. Chem.* **1980**, *52*, 733. Buchwald, S. L.; La Maire, S. J.; Nielsen, R. B.; Watson, B. T.; King, S. M. *Tetrahedron Lett.* **1987**, *28*, 3895.

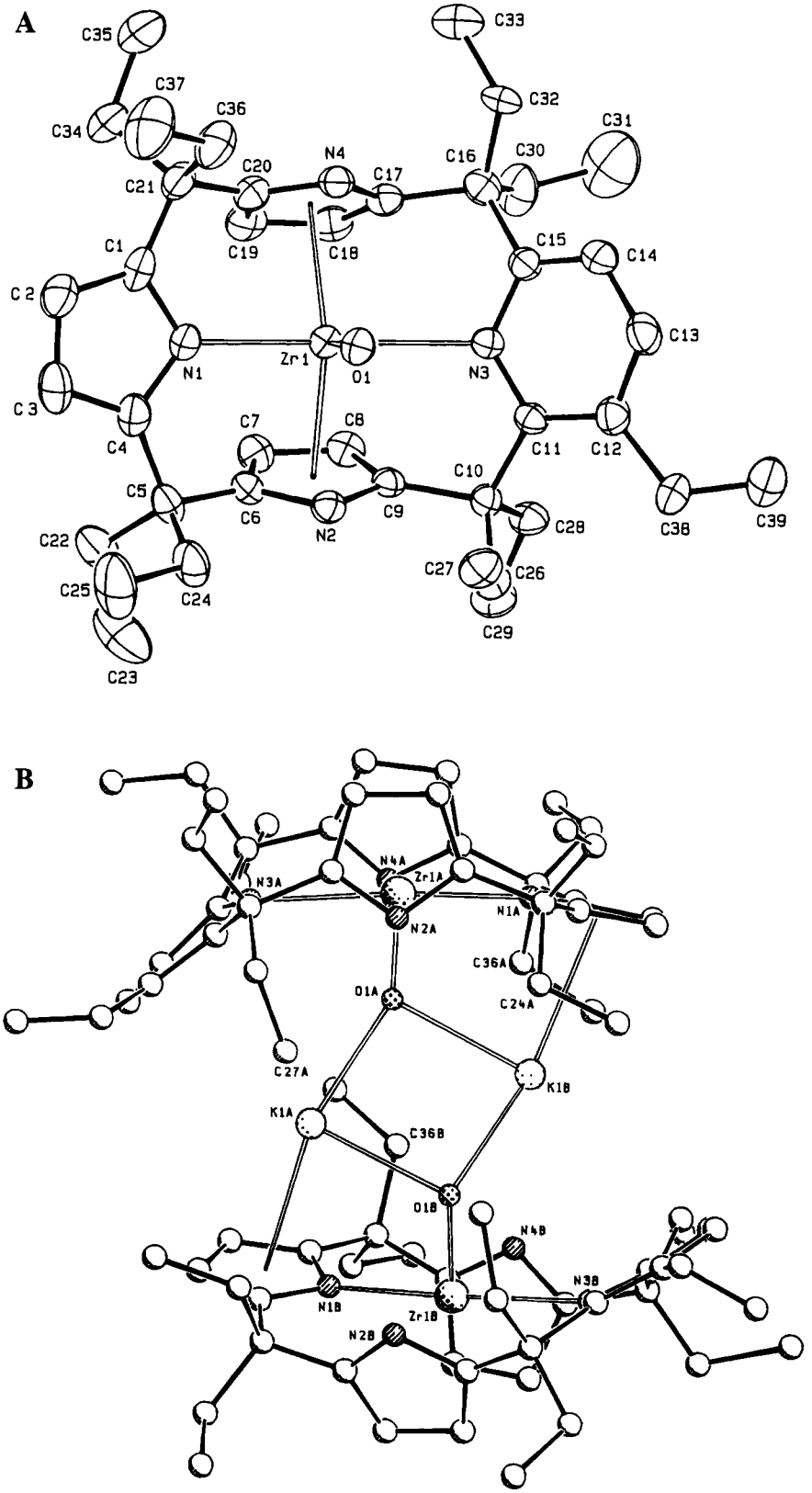

Figure 1. (A) ORTEP drawing of the anion in complex **8** (molecule A) (30% probability ellipsoids). (B) A SCHAKAL perspective view of the dimer in complex **8**.

2). Each of them is further engaged in relatively short contacts with two C–H bonds of the *meso* ethyl groups: K1A···C27A, 3.338(8), K1A···H271A, 2.91 Å; C27A–H271A···K1A, 103°; K1A···C36B, 3.488(8); K1A···H361B, 2.78 Å; C36B–H361B···K1A, 117°; K1B···C24A, 3.716(8), K1B···H242A, 2.88 Å; C24A–H242A···K1B, 132°; K1B···C36A, 3.602(8); K1B···H361A, 2.95 Å; C36A–H361A···K1B, 125°.

Reactions in Schemes 2 and 4 follow, very probably, the same mechanism discussed earlier. The use, however, of the zirconium–ethyl and –vinyl derivatives allowed us to define the regiochemistry of the homologation reaction. In all cases we found, regardless of the substituent, both in the solid state and in solution, the substitution of the *meta* position in the pyridine ring. Such a regiochemistry is in agreement with that observed

Table 1. Experimental Data for the X-ray Diffraction Studies on Crystalline Compounds **8**, **13**, **17**, and **19**

	8	**13**	**17**	**19**
chemical formula	$C_{78}H_{106}K_2N_8O_2Zr_2$	$C_{38}H_{51}N_4NbO{\cdot}0.25(C_6H_{14})$	$C_{38}H_{52}HfN_4$	$C_{39}H_{53}N_4$
a (Å)	13.763(3)	29.380(5)	11.459(3)	13.038(3)
b (Å)	14.464(2)	13.467(4)	13.140(3)	18.859(3)
c (Å)	19.276(3)	40.862(7)	23.454(4)	14.805(3)
α (deg)	82.77(1)	90	90	90
β (deg)	89.71(2)	107.55(2)	102.23(3)	102.80(2)
γ (deg)	76.52(1)	90	90	90
V (Å^3)	3700.7(11)	15415(6)	3451.4(14)	3549.8(13)
Z	2	16	4	4
fw	1448.4	694.3	743.3	578.9
space group	$P\bar{1}$	$C2/c$	$P2_1/n$	$P2_1/n$
t (°C)	22	22	22	22
λ (Å)	1.71069	0.71069	0.71069	1.54178
ϱ_{calcd} (g cm^{-3})	1.300	1.197	1.431	1.083
μ (cm^{-1})	4.37	3.30	30.25	4.49
transmn coeff	0.918−1.000	0.983−1.000	0.888−1.000	0.668−1.000
R^a	0.045	0.047	0.026	0.057
$R_w{}^b$	0.044		0.027	0.067
w$R2^c$		0.098		

$^a R = \Sigma||\Delta F|/\Sigma|F_o||$. $^b R_w = \Sigma w^{1/2}|\Delta F|/\Sigma w^{1/2}|F_o|$. ^{c} wR2 $= [\Sigma(w\Delta F^2)^2/\Sigma(wF_o^2)^2]^{1/2}$.

Table 2. Selected Interatomic Distances (Å) and Angles (deg) for Complex **8**

	mol. A	mol. B		mol. A	mol. B
		(A) In the Zirconyl Moiety			
Zr1−O1	1.802(5)	1.806(4)	N4−C17	1.371(8)	1.328(9)
Zr1−N1	2.243(6)	2.257(5)	N4−C20	1.363(9)	1.340(10)
Zr1−N2	2.521(5)	2.522(4)	C1−C2	1.398(10)	1.380(9)
Zr1−N3	2.525(4)	2.551(5)	C2−C3	1.406(13)	1.391(10)
Zr1−N4	2.471(6)	2.452(6)	C3−C4	1.409(10)	1.374(8)
Zr1−C6	2.580(6)	2.578(6)	C4−C5	1.528(11)	1.502(8)
Zr1−C7	2.682(7)	2.653(6)	C5−C6	1.502(8)	1.514(7)
Zr1−C8	2.648(7)	2.611(6)	C6−C7	1.394(8)	1.390(8)
Zr1−C9	2.525(6)	2.508(5)	C7−C8	1.421(9)	1.407(8)
Zr1−C17	2.577(6)	2.598(8)	C8−C9	1.403(9)	1.391(9)
Zr1−C18	2.752(6)	2.758(8)	C9−C10	1.540(8)	1.499(8)
Zr1−C19	2.711(8)	2.744(9)	C10−C11	1.527(8)	1.550(9)
Zr1−C20	2.556(6)	2.573(8)	C11−C12	1.399(9)	1.421(10)
Zr1−Cp2	2.304(6)	2.291(6)	C12−C13	1.389(10)	1.363(11)
Zr1−Cp4	2.335(6)	2.346(8)	C13−C14	1.392(11)	1.364(11)
N1−C1	1.383(9)	1.366(7)	C14−C15	1.371(11)	1.392(12)
N1−C4	1.376(9)	1.379(8)	C15−C16	1.528(9)	1.532(10)
N2−C6	1.379(9)	1.375(8)	C16−C17	1.513(10)	1.490(11)
N2−C9	1.379(7)	1.364(6)	C17−C18	1.379(10)	1.439(13)
N3−C11	1.361(7)	1.339(9)	C18−C19	1.413(10)	1.408(10)
N3−C15	1.358(9)	1.365(10)	C19−C20	1.406(10)	1.431(13)
Cp2−Zr1−Cp4	127.7(2)	129.0(2)	Zr1−N1−C1	124.1(5)	125.6(4)
N3−Zr1−Cp4	91.8(2)	91.5(2)	C1−N1−C4	108.2(6)	107.0(4)
N3−Zr1−Cp2	89.9(2)	89.6(2)	Zr1−N2−C9	74.3(3)	73.7(3
N1−Zr1−Cp4	90.4(2)	89.5(2)	Zr1−N2−C6	76.7(3)	76.6(3)
N1−Zr1−Cp2	91.7(2)	91.4(2)	C6−N2−C9	106.7(5)	107.5(4)
N1−Zr1−N3	175.7(2)	177.8(2)	Zr1−N3−C15	113.1(3)	116.1(4)
O1−Zr1−Cp4	117.2(2)	116.1(2)	Zr1−N3−C11	117.2(3)	117.9(4)
O1−Zr1−Cp2	115.0(2)	114.9(2)	C11−N3−C15	120.9(5)	120.5(6)
O1−Zr1−N3	84.0(2)	85.8(2)	Zr1−N4−C20	77.7(4)	79.6(4)
O1−Zr1−N1	91.6(2)	92.0(2)	Zr1−N4−C17	78.5(4)	80.9(4)
Zr1−N1 −C4	126.6(5)	126.3(4)	C17−N4−C20	106.7(5)	111.1(6)
		(B) In the K^+ Sphere			
K1A−O1A		2.529(5)	K1B−O1A		2.659(4)
K1A−O1B		2.677(3)	K1B−O1B		2.564(4)
K1A−N1B		2.919(5)	K1B−N1A		3.004(5)
K1A−C1B		3.041(7)	K1B−C1A		3.172(7)
K1A−C2B		3.267(8)	K1B−C2A		3.413(9)
K1A−C3B		3.293(7)	K1B−C3A		3.407(9)
K1A−C4B		3.101(7)	K1B−C4A		3.159(9)
K1A−O1A−K1B		94.8(1)	K1A−O1B−K1B		93.5(1)
Zr1A−O1A−K1B		115.1(2)	Zr1B−O1B−K1B		130.0(2)
Zr1A−O1A−K1A		147.9(2)	Zr1B−O1B−K1A		112.5(2)

in the reaction of the free pyrrole with carbenes.[12] Another important consequence of the reaction shown in Scheme 6 is the possibility of introducing a reactive functional group, *i.e.*, vinyl, in the periphery of the macrocycle. The general applicability of the reaction route in Scheme 4 has been proven by its extension to several alkyl derivatives. The reaction works

Scheme 5

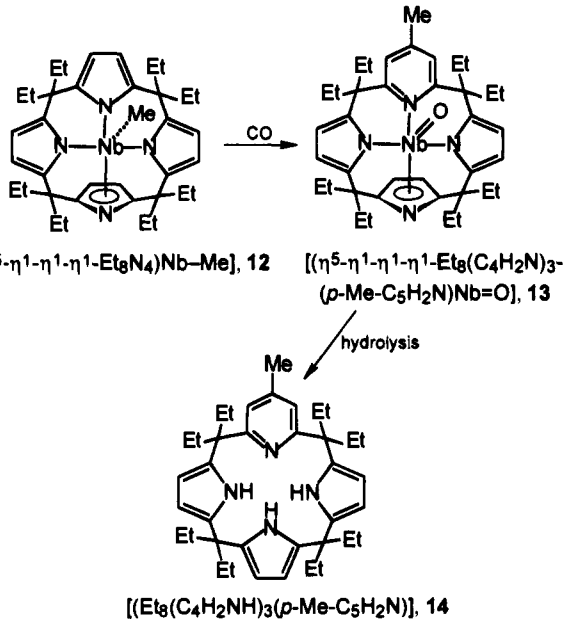

[(η^5-η^1-η^1-η^1-Et_8N_4)Nb–Me], **12**

[(η^5-η^1-η^1-η^1-$Et_8(C_4H_2N)_3$-(*p*-Me-C_5H_2N)Nb=O], **13**

[($Et_8(C_4H_2NH)_3$(*p*-Me-C_5H_2N)], **14**

regardless of the nature of the alkyl group and of the alkali cation.

Attempts to modify the regiochemistry of the homologation of the *meso*-octaethylporphyrinogen, [$Et_8N_4H_4$], and to proceed further with the homologation of a second pyrrole ring have been successfully negotiated using metals other than zirconium. For instance, the use of niobium allowed a modification of the regiochemistry of the substitution at the pyridine ring in the homologation of [$Et_8N_4H_4$] to the corresponding trispyrrole–monopyridine macrocycle. This has been performed according to Scheme 5.

The synthesis of **12** has been achieved following conventional procedures (see the Experimental Section).

The reaction of **12** with carbon monoxide parallels the reaction we observed in the case of zirconium, since both metals have very oxophilic properties and generate η^2-acyls. Thus, we observe the cleavage of the C=O bond,[3] the formation of the oxoniobium(V) fragment, and the homologation of one of the pyrrolyl anions to the 4-methylpyridine fragment.[12]

Complex **13** has been fully characterized (see Experimental Section), including an X-ray analysis (Figure 2). The diagnostic Nb=O infrared stretch appears at 908 cm^{-1}.[17] Although rare examples of porphyrin-type complexes have been reported,[18] the porphyrinogen and porphyrinogen derivatized macrocycle are particularly suitable for the stabilization of high-valent metals.[10] The mechanism of the pyrrole to pyridine[12] homologation should be quite similar to that which we reported in Scheme 6, although assisted by zirconium in that case. However, a major difference is the change in the regiochemistry of the reaction encountered on moving to niobium. The formation of a *para*-substituted pyridine is believed to be derived from the electrophilic attack of the acyl carbenium ion to the β position of the pyrrole.

(17) Hubert-Pfalzgraf, L. G.; Postel, M.; Riess, J. G. In *Comprehensive Coordination Chemistry*; Wilkinson, G., Gillard, R. D., McCleverty, J. A., Eds.; Pergamon: Oxford, 1987; Vol. 3, Chapter 34.

(18) (a) Lecompte, C.; Protas, J.; Guilard, R.; Fliniaux, B.; Fournari, P. *J. Chem. Soc., Dalton Trans.* **1979**, 1306; *J. Chem. Soc., Chem. Commun.* **1976**, 434. (b) Lecompte, C.; Protas, J.; Richard, P.; Barbe, J. M.; Guilard, R. *J. Chem. Soc., Dalton Trans.* **1982**, 247. (c) Gouterman, M.; Hanson, L. K.; Khalil, G. E.; Bucher, J. W.; Rohbock, K.; Dolphin, D. *J. Am. Chem. Soc.* **1975**, *97*, 3142. (d) Green, M. L. H.; Moreau, J. J. *Inorg. Chim. Acta* **1978**, *31*, L461.

Scheme 6

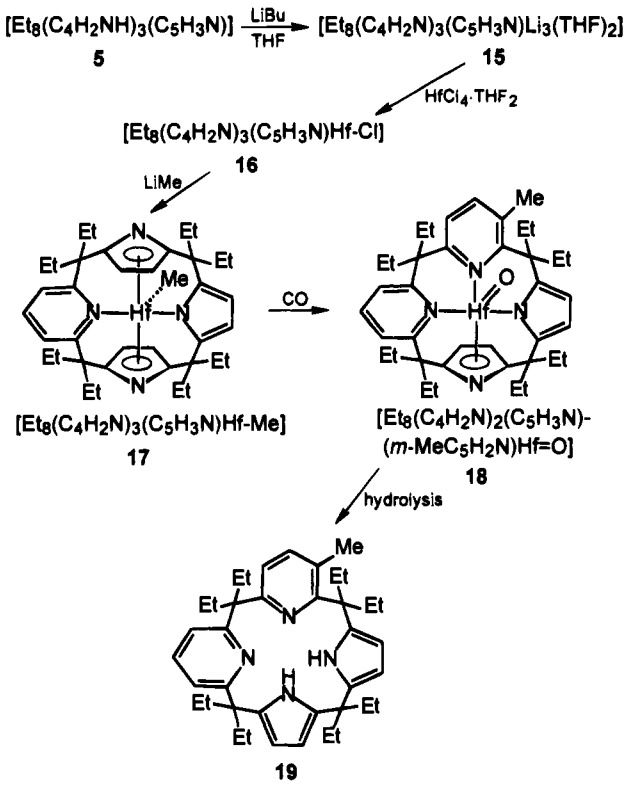

19

The regiochemistry determined by niobium is different from that imposed by zirconium and may be due to a different orientation and bonding mode of the pyrrole to the metal. An η^3-bonding mode of the pyrrolyl anion to niobium may be responsible for orientating the pyrrole β-carbon into a position susceptible to electrophilic attack and thus for the formation of a *p*-methylpyridine instead of a *meta*-substituted pyridine. This explanation emphasizes the ability of the pyrrolyl anion in the porphyrinogen complexes to display different bonding modes and to fluctuate within a complex.[5]

The novel ligand **14** containing the *p*-methylpyridine fragment is obtained quantitatively from a controlled hydrolysis of **13**. The structure of **13** and, in particular, the bonding mode of the trispyrrole–monopyridine ligand will be discussed jointly with the structure of **17**, since such a bonding mode is a critical factor for its further reactivity.

The full success of the homologation of a pyrrole into a pyridine ring shown in Schemes 2, 4, and 5 using our methodologies prompted us to extend them to the second homologation (see Scheme 1) of porphyrinogen to a bispyrrole–bispyridine macrocycle. For the second homologation, we proceeded as reported in Scheme 6 and as described in detail in the Experimental Section.

The lithiation of the trispyrrole–monopyridine derivative **5** and the metalation of **15** with $HfCl_4$·THF_2 were carried out as reported for the *meso*-octaethylporphyrinogen.[5-7] We were unable to free **16** from LiCl, due to its insolubility; however, this did not affect the alkylation reaction leading to **17**. The reaction of **17** with carbon monoxide is slow, and the corresponding hafnium derivative ($\nu_{Hf=O}$, 826 cm^{-1}) has been isolated. The high insolubility of **18**, however, precluded analysis by X-ray diffraction or NMR spectroscopy. The η^1-η^5 bonding mode of the two pyrrolyl anions to the metal in **18** has been proposed on the basis of the structure of **17** and on the fact that we never observed in porphyrinogen–metal complexes any case in which two vicinal pyrroles are η^5-bonded

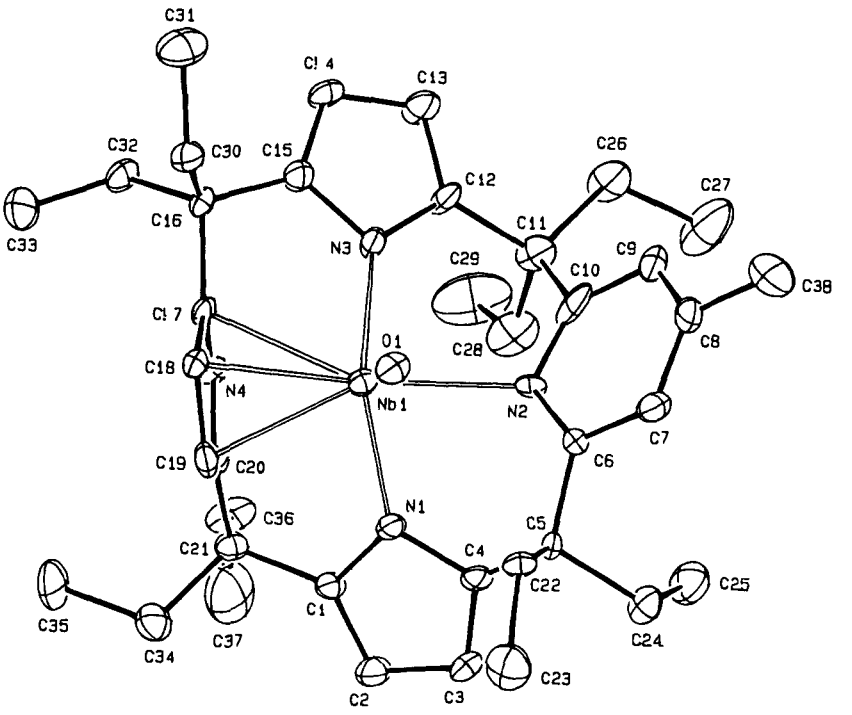

Figure 2. ORTEP drawing of complex **13** (molecule A) (30% probability ellipsoids).

Scheme 7

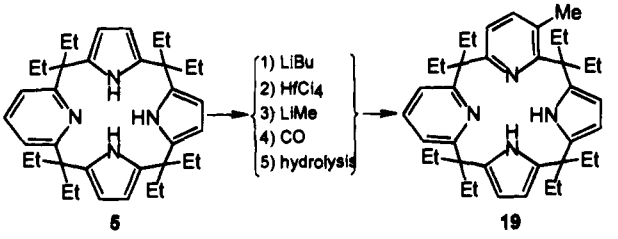

to the metal. The hydrolysis of **18** to **19** does not require the isolation of **18**, and the carbonylation of **17** can be directly followed by the hydrolysis to **19** (see Experimental Section). Therefore, the conversion of **5** to **19**, corresponding to the second homologation of the porphyrinogen skeleton, can be summarized as in Scheme 7.

The first step requires the use of $HfCl_4$ instead of $ZrCl_4$. This was mainly dictated by the fact that, empirically, complexes like **17** and **18** were unobtainable, especially the carbonylation step, using zirconium. It could be that the acidity and the oxophilicity of hafnium *vs* zirconium is much more favorable for these transformations.[19] The regiochemistry of the second homologation displayed in Schemes 6 and 7 deserves comment. We can assume that the hafnium-assisted homologation mechanism is quite similar to that observed in the case of the first homologation assisted by zirconium.

Among the two positional isomers with the methyl group in the two possible nonequivalent *meta* positions, that shown has been the only one identified. The selective formation of only one regioisomer having two *cis* pyridine rings (see compound **III** in Scheme 1) aids our understanding of the homologation mechanism. On the basis of the structure of **17** in the solid state, which is supported by the solution structure as observed by ^1H NMR spectroscopy, the homologation occurs only on the η^5-bonded pyrrole and thus leads exclusively to the *cis* isomer **III** (Scheme 1). It seems very likely that the η^5-pyrrolyl

(19) Fay, R. C. In *Comprehensive Coordination Chemistry*; Wilkinson, G., Gillard, R. D., McCleverty, J. A., Eds.; Pergamon: Oxford, 1987; Vol. 3, Chapter 32.

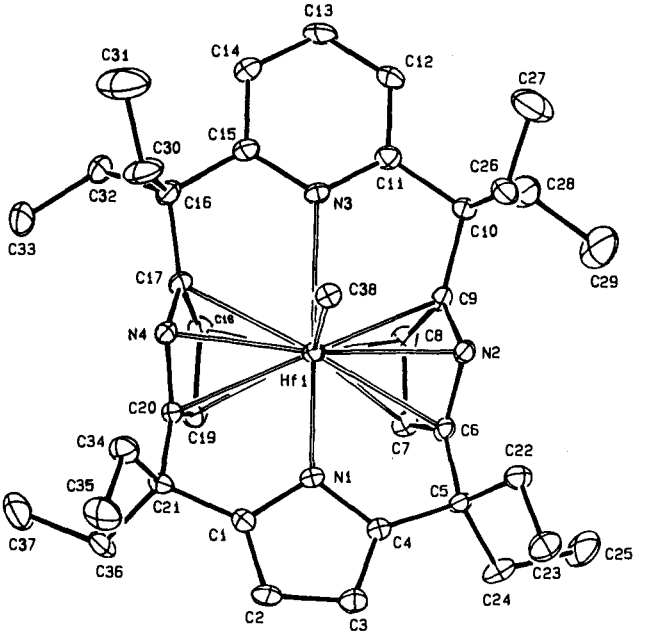

Figure 3. ORTEP drawing of complex **17** (molecule A) (30% probability ellipsoids).

anions have the appropriate orientation and the geometrical proximity for a facile attack by the carbenoid species formed from the carbon monoxide insertion. The regiochemistry of both homologation reactions depends on the bonding mode of the ligand, which is directly determined by the nature of the transition metal. In this context, we will jointly discuss the solid state structures of **13** and **17**, both containing the trispyrrole–monopyridine ligand, as shown in Figures 2 and 3, respectively. The most significant differences between the two complexes are the bonding modes of the ligand. In complex **13**, the metal is η^5-bonded to the pyrrolyl anion *trans* to the η^1-pyridine, with the other two pyrroles η^1-bonded. In complex **17**, however, hafnium is η^5-bonded to two *trans* pyrroles and η^1-bonded to the pyridine ring *trans* to a η^1-pyrrole. The significantly different conformations of the ligand, derived from the differing

Table 3. Selected Bond Distances (Å) and Angles (deg) for Complex **13**

	mol. A	mol. B		mol. A	mol. B
Nb1–O1	1.710(4)	1.706(4)	C3–C4	1.365(10)	1.376(9)
Nb1–N1	2.106(4)	2.106(5)	C4–C5	1.492(11)	1.494(10)
Nb1–N2	2.355(5)	2.370(5)	C5–C6	1.504(9)	1.550(9)
Nb1–N3	2.145(6)	2.127(6)	C5–C22	1.572(11)	1.547(12)
Nb1–N4	2.407(6)	2.401(6)	C5–C24	1.554(8)	1.566(8)
Nb1–C17	2.400(6)	2.383(6)	C6–C7	1.389(11)	1.377(10)
Nb1–C18	2.547(7)	2.512(7)	C7–C8	1.378(11)	1.387(10)
Nb1–C19	2.497(7)	2.494(7)	C8–C9	1.382(13)	1.365(11)
Nb1–C20	2.441(7)	2.454(6)	C8–C38	1.528(13)	1.507(10)
Nb1–Cp4	2.163(6)	2.149(6)	C9–C10	1.421(12)	1.374(11)
N1–C1	1.376(9)	1.395(9)	C10–C11	1.545(10)	1.517(11)
N1–C4	1.400(8)	1.406(8)	C11–C12	1.514(8)	1.498(8)
N2–C6	1.318(9)	1.352(10)	C12–C13	1.356(8)	1.398(11)
N2–C10	1.342(9)	1.363(10)	C13–C14	1.405(10)	1.400(10)
N3–C12	1.368(9)	1.358(9)	C14–C15	1.361(10)	1.370(11)
N3–C15	1.378(7)	1.418(8)	C15–C16	1.513(10)	1.491(10)
N4–C17	1.388(9)	1.390(8)	C16–C17	1.519(9)	1.508(9)
N4–C20	1.323(8)	1.341(9)	C17–C18	1.368(10)	1.388(12)
C1–C2	1.359(9)	1.355(8)	C18–C19	1.401(10)	1.389(8)
C1–C21	1.529(8)	1.510(9)	C19–C20	1.392(12)	1.425(12)
C2–C3	1.432(10)	1.437(10)	C20–C21	1.513(11)	1.521(9)
N2–Nb1–N3	83.6(2)	82.4(2)	Nb1–N1–C4	127.0(4)	126.3(4)
N1–Nb1–O1	107.0(2)	107.3(2)	Nb1–N1–C1	125.7(4)	126.2(4)
N1–Nb1–N3	83.6(2)	82.4(2)	C1–N1–C4	107.3(5)	107.4(5)
N1–Nb1–N2	76.3(2)	76.1(2)	Nb1–N2–C10	118.2(4)	119.3(4)
Cp4–Nb1–O1	106.9(2)	107.8(3)	Nb1–N2–C6	112.8(4)	118.8(4)
Cp4–Nb1–N3	96.7(2)	96.9(3)	C6–N2–C10	117.5(6)	118.4(6)
Cp4–Nb1–N2	168.6(2)	166.1(2)	Nb1–N3–C15	122.4(4)	122.3(4)
Cp4–Nb1–N1	96.2(2)	95.7(2)	Nb1–N3–C12	132.4(4)	132.2(5)
N3–Nb1–O1	107.2(2)	107.2(2)	C12–N3–C15	105.2(5)	105.4(5)
N2–Nb1–O1	83.7(2)	85.5(2)			

Table 4. Selected Bond Distances (Å) and Angles (deg) for Complex **17**

Hf1–N1	2.189(4)	N4–C20	1.377(6)
Hf1–N2	2.484(5)	C1–C2	1.362(7)
Hf1–N3	2.708(4)	C1–C21	1.506(6)
Hf1–N4	2.491(5)	C2–C3	1.415(7)
Hf1–C6	2.521(4)	C3–C4	1.376(7)
Hf1–C7	2.553(5)	C4–C5	1.509(7)
Hf1–C8	2.535(5)	C5–C6	1.523(7)
Hf1–C9	2.502(5)	C6–C7	1.402(7)
Hf1–C17	2.505(4)	C7–C8	1.418(7)
Hf1–C18	2.529(5)	C8–C9	1.392(7)
Hf1–C19	2.548(5)	C9–C10	1.530(7)
Hf1–C20	2.516(5)	C10–C11	1.520(6)
Hf1–C38	2.268(4)	C11–C12	1.389(7)
Hf1–Cp2	2.221(5)	C12–C13	1.366(6)
Hf1–Cp4	2.221(5)	C13–C14	1.375(7)
N1–C1	1.401(7)	C14–C15	1.391(7)
N1–C4	1.394(6)	C15–C16	1.515(7)
N2–C6	1.378(6)	C16–C17	1.517(6)
N2–C9	1.386(6)	C17–C18	1.396(7)
N3–C11	1.358(7)	C18–C19	1.429(7)
N3–C15	1.348(6)	C19–C20	1.408(7)
N4–C17	1.374(7)	C20–C21	1.519(7)
N2–Hf1–N3	88.4(1)	Hf1–N1–C4	127.2(3)
N1–Hf1–C38	93.1(2)	Hf1–N1–C1	127.2(3)
N1–Hf1–N3	173.5(1)	C1–N1–C4	105.6(4)
N1–Hf1–N2	91.1(2)	C6–N2–C9	105.5(4)
Cp2–Hf1–C38	112.0(2)	Hf1–N2–C9	74.6(3)
Cp2–Hf1–N3	88.5(2)	Hf1–N2–C6	75.5(3)
Cp2–Hf1–N1	94.2(2)	Hf1–N3–C15	120.5(3)
Cp4–Hf1–C38	110.7(2)	Hf1–N3–C11	120.3(3)
Cp4–Hf1–N3	88.3(2)	C11–N3–C15	119.0(4)
Cp4–Hf1–N1	93.9(2)	C17–N4–C20	106.5(4)
N1–Hf1–C38	93.1(1)	Hf1–N4–C20	75.0(3)
N3–Hf1–C38	80.4(1)	Hf1–N4–C17	74.6(3)

ligand bonding modes imposed by the metal, are demonstrated by the structural parameters listed in Table 6, which should be compared with those of the free ligand **5**.[7a]

Table 5. Selected Bond Distances (Å) and Angles (deg) for Compound **19**

N1–C1	1.374(8)	C8–C9	1.377(9)
N1–C4	1.390(9)	C9–C10	1.493(9)
N2–C6	1.368(8)	C10–C11	1.558(10)
N2–C9	1.373(10)	C11–C12	1.407(11)
N3–C11	1.335(8)	C12–C13	1.370(10)
N3–C15	1.338(8)	C12–C39	1.503(9)
N4–C17	1.352(8)	C13–C14	1.397(10)
N4–C21	1.361(8)	C14–C15	1.385(11)
C1–C2	1.388(10)	C15–C16	1.522(8)
C1–C22	1.520(10)	C16–C17	1.513(8)
C2–C3	1.428(9)	C17–C18	1.387(10)
C3–C4	1.371(11)	C18–C19	1.381(10)
C4–C5	1.518(9)	C19–C20	1.406(10)
C5–C6	1.511(11)	C20–C21	1.386(10)
C6–C7	1.374(11)	C21–C22	1.533(10)
C7–C8	1.395(11)		
C1–N1–C4	110.7(6)	C11–N3–C15	120.6(5)
C6–N2–C9	110.9(6)	C17–N4–C21	119.1(5)

In complex **13**, the macrocycle assumes a very irregular shape which cannot be described as a saddle conformation. The four nitrogen atoms lie nearly in a plane for molecule A (Figure 2), while they show remarkable tetrahedral distortions in molecule B (the two independent molecules A and B have similar overall geometries). The niobium atom is strongly displaced by the N_4 plane toward the oxygen atom. The η^5-bonded pyrrole ring (D) is nearly perpendicular to the N_4 plane, while the opposite pyridine rings and the σ-bonded pyrrole rings are midway between being parallel and perpendicular to that plane. In addition, the two opposite pyrrole rings are twisted away from each other, removing the saddle shape conformation (Table 6).

The additional structurally relevant parameters are the Nb=O distance [1.710(4) Å],[18] quite close to that of other oxoniobium(V) derivatives, and the Hf–Me bond distance [2.268(4) Å], which falls in the usual Hf–C single bond range.[2d]

Table 6. Comparison of Structural Parameters for Compounds **8**, **13**, **17**, and **19** (M = Zr for **8**, M = Nb for **13**, M = Hf for **17**)

		8[a]	13[a]	17	19
dist of atoms from N_4 core, Å	N1	−0.001(5) [−0.020(4)]	0.011(5) [0.033(4)]	0.089(4)	0.056(6)
	N2	0.001(5) [0.018(4)]	−0.012(5) [−0.037(4)]	−0.083(4)	−0.056(6)
	N3	−0.001(5) [−0.021(5)]	0.012(5) [0.037(4)]	0.077(4)	0.034(5)
	N4	0.002(6) [0.034(6)]	−0.010(5) [−0.033(4)]	−0.083(4)	−0.035(5)
	M	0.089(1) [−0.067(1)]	0.765(1) [0.793(1)]	0.221(1)	
dist of M from A, Å[b]		0.384(1) [0.429(1)]	−0.121(1) [0.142(1)]	−0.011(1)	
dist of M from B, Å		2.297(1) [2.286(1)]	1.684(1) [1.583(1)]	2.221(1)	
dist of M from C, Å		1.550(1) [1.226(1)]	0.086(1) [0.084(1)]	−0.132(1)	
dist of M from D, Å		2.314(1) [2.321(1)]	−2.160(1) [−2.144(1)]	−2.220(1)	
dihedral angles between the N_4 core	A	167.3(2) [167.3(1)]	151.1(2) [154.6(2)]	176.4(1)	76.7(2)
and the A,B,C,D rings, deg	B	68.1(2) [67.4(2)]	35.9(2) [36.4(2)]	110.4(1)	150.9(2)
	C	141.1(1) [149.9(2)]	144.1(2) [142.1(2)]	179.8(2)	89.8(2)
	D	71.5(2) [73.0(2)]	85.5(2) [85.1(2)]	110.6(1)	102.0(2)
dihedral angles between A, C rings			61.4(3) [61.8(3)]	3.7(2)	13.1(2)
dihedral angles between B, D rings			59.1(3) [63.4(2)]	41.6(2)	75.1(2)

[a] Molecule B in square brackets. [b] A, B, C, and D refer to the pyrrole or pyridine rings containing N1, N2, N3, and N4, respectively.

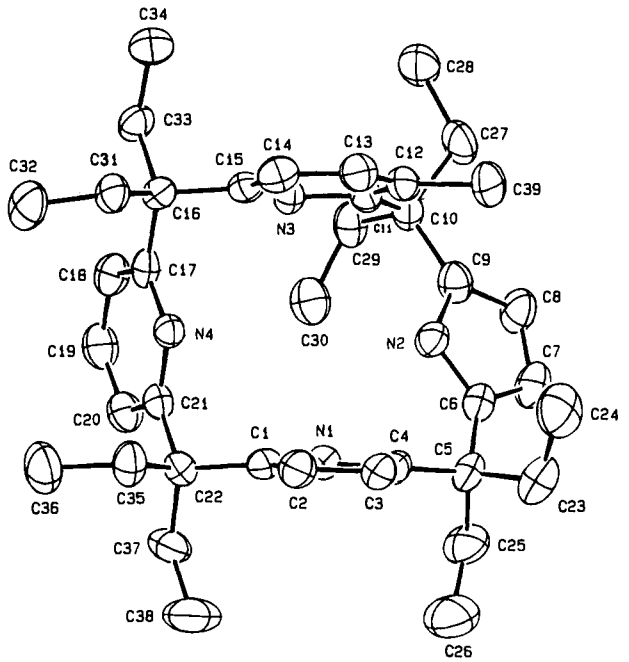

Figure 4. ORTEP drawing of compound **19** (30% probability ellipsoids).

The structural proof for the double homologation of the porphyrinogen skeleton is provided by an X-ray analysis of **19** (Figure 4). The orientation of the rings with respect to the N_4 plane is remarkably different, as can be seen from the dihedral angles given in Table 6. The two opposite rings A and C are nearly parallel with each other and nearly perpendicular to the mean plane through the nitrogen atoms. The two opposite rings B and D are approximately perpendicular to each other, the first one being midway between being parallel and perpendicular to the N_4 plane, the second one being nearly perpendicular. The two pairs are oriented toward the opposite sides of the N_4 plane.

Conclusions

The homologation of a pyrrole ring within a macrocyclic structure can be achieved when it is bonded to an oxophilic metal which is able to form an η^2-formyl or η^2-acyl carbenium ion from the insertion of carbon monoxide into metal−hydrogen and metal−carbon bonds. The cleavage of the oxygen−carbon bond is driven by the formation of stable metal−oxo complexes which provides the appropriate "CH" or "CR" fragment for the homologation reaction. This occurs with the formation of a *meta*- or *para*-substituted pyridine ring depending on the nature of the metal: Zr and Hf give the *meta*, while Nb leads to the *para* derivatives. The regiochemistry of the reaction seems to depend on the bonding mode (η^3 or η^5) of the pyrrolyl anion to the metal. The formation of the *cis*-bispyridine derivative in the homologation reaction of the *meso*-octaethyltrispyrrole−monopyridine macrocycle is also controlled by the bonding mode of the macrocycle ligand, the η^5-bonded pyrrolyl anion being the only one to undergo a ring-opening reaction. The results reported emphasize how we can modify the skeleton and control the related regiochemistry of rather complex structures, like those of macrocyclic polypyrrole, using organometallic methodologies. In addition, this does not remain just a chemical curiosity, since we can carry this transformation as a good preparative method for a novel class of macrocycles. The introduction of one or two pyridines into a tetrapyrrolic macrocycle greatly modifies the geometric and electronic properties of this very important class of compounds.

Experimental Section

General Procedure. All reactions were carried out under an atmosphere of purified nitrogen. Solvents were dried and distilled before use by standard methods. Syntheses of complexes **1**,[5a] **2**[5a], and **3**[7a] have been recently reported.[5a] Syntheses of alkyl derivatives **6** and **7** are very similar to those reported in ref 5a. Infrared spectra were recorded with a Perkin-Elmer 883 spectrophotometer, and ^{1}H NMR spectra were measured on a 200-AC Bruker instrument.

Preparation of 4. A toluene (100 mL) suspension of **3** (2.00 g, 3.0 mmol) was stirred under CO for 30 h, until gas absorption stopped. A white microcrystalline suspension was obtained, which was filtered and dried (78%). White crystals were obtained by recrystallization from toluene. Anal. Calcd for $C_{37}H_{49}KN_4OZr$: C, 63.84; H, 7.09; N, 8.05. Found: C, 63.76; H, 7.10; N, 7.82. IR (Nujol): ν(Zr=O) 780 cm^{-1}. ^{1}H NMR (C_6D_6): δ 0.50−1.40 (m, CH_3, 24 H), 1.65−2.62 (m, CH_2, 16 H), 5.52−6.42 (s, C_4H_2N, 6 H), 6.80−7.60 (m, C_5H_4N, 3 H).

Preparation of 5. Method A. A toluene (100 mL) suspension of **3** (5.65 g, 8.46 mmol) was stirred under CO for 5 days, until gas absorption stopped. Water (30 mL) was added, and the mixture was stirred for 1 h. The suspension was filtered, and the organic phase was separated and dried over Na_2SO_4. Toluene was evaporated to dryness and *n*-pentane added (100 mL); a small amount of solid was removed by filtration and the filtrate was evaporated to dryness. An orange microcrystalline product was obtained (90%). White crystals were obtained by recrystallization from *n*-pentane. Anal. Calcd for $C_{37}H_{52}N_4$: C, 80.39; H, 9.48; N, 10.13. Found: C, 80.46; H, 9.70; N, 10.02. ^{1}H NMR (CD_2Cl_2): δ 0.58 (t, CH_3, 12 H), 0.63 (t, CH_3, 12 H), 1.75 (q, CH_2, 4 H), 1.76 (q, CH_2, 4 H), 2.02 (q, CH_2, 4 H), 2.18 (q, CH_2, 4 H), 5.87 (t, pyrrole, 6 H, J = 2.80 Hz), 6.78 (s, NH, 2 H), 7.18 (d, pyridine, 2 H, J = 7.80 Hz), 7.19 (s, NH, 1 H), 7.57 (t, pyridine, 1 H, J = 7.80 Hz).

Large Scale One-Pot Type Synthesis of 5 Using KH. Bu^{n}Li (500 mL, 1.6 M in hexane, 800.0 mmol) was added to a THF (350 mL)

solution of $Et_8N_4H_4$ (108 g, 200.0 mmol). The mixture was heated for 2 h at 50 °C, and then the solvent was evaporated to dryness; the residue was washed with *n*-hexane (500 mL) and filtered. The solid was dissolved in toluene (600 mL), $ZrCl_4(THF)_2$ (66.0 g, 175.0 mmol) added, and the mixture stirred overnight at room temperature, followed by 1 h at 60 °C. LiCl was removed by filtering the hot solution. The clear yellow solution was treated with KH (7.0 g, 175 mmol) and heated under vacuum at 90−100 °C for 4 days. A white solid formed, **3**, (potassium zirconium hydride complex), which was filtered while hot and dried (70%). The complex so obtained was dissolved in THF (400 mL) and stirred under CO at room temperature for 12 h, until gas absorption stopped. The solvent was evaporated to dryness, and the residue was treated with toluene (500 mL) in the air. Water (200 mL) was slowly added and the solution was stirred for 2 h. ZrO_2 was filtered off and washed with toluene (200 mL). The organic phase was separated and dried over Na_2SO_4. Toluene was evaporated to dryness and the residue was recrystallized from methanol or acetonitrile gave **7** as a white crystalline solid (42 g, 38%).

Large Scale One-Pot Type Synthesis of 5 Using NaH. Bu^nLi (300 mL, 1.6 M in hexane, 480 mmol) was added to a THF (300 mL) solution of $Et_8N_4H_4$ (64.8 g, 120 mmol). The mixture was heated for 2 h at 50 °C, and then the solvent was evaporated to dryness; the residue was washed with *n*-hexane (500 mL) and filtered. The white crystalline solid was dissolved in toluene (600 mL), $ZrCl_4(THF)_2$ (35 g, 100 mmol) added, and the mixture left to stir for 15 h at room temperature. LiCl formed and was filtered off while the solution was hot. The clear yellow solution was treated with NaH (2.60 g, 108 mmol) and heated under vacuum at 100 °C for 3 days and then cooled and stirred under CO at room temperature for 1 h while the addition of CO was continued. Stirring was continued further for 15 h. Water (200 mL) was then slowly added, and the mixture was stirred for another 6 h. ZrO_2 was filtered off and washed with toluene (200 mL). The organic phase was separated and dried over Na_2SO_4. Toluene was evaporated to dryness, and the residue was recrystallized twice from acetonitrile to give **7** as a crystalline solid (39 g, 58.8%).

N.B. Sometimes the homologation of pyrrole in pyridine may be incomplete and a non-negligible amount of tetrapyrrole may be detectable. In that case the crystallization of the final product **5** may be difficult. In such a case we recommend that the previous preparation be dissolved in warm hexane and an aqueous solution of HCl should be added in a 1:1 HCl:ligand ratio. The chlorohydrate of **5** forms as a yellow crystalline solid. After 1 h of stirring the mixture, the solid is filtered, washed with *n*-hexane, and suspended again in hexane. A 1:1 KOH:water solution should then be added and the mixture heated to 60−70 °C for 1 h. The solid dissolves in the *n*-hexane phase which is then dried over Na_2SO_4. The solvent should be evaporated to dryness and the solid recrystallized from acetonitrile to give pure **5**.

Preparation of 8. A suspension of **6** (2.40 g, 3.40 mmol) in toluene (50 mL) was stirred under a CO atmosphere at room temperature for 1 day. The absorption was rather slow and produced a yellow solution. The solvent was evaporated to dryness, and the solid was washed with *n*-hexane (73%). The recrystallization carried out in toluene−hexane gave light yellow crystals. Anal. Calcd for $C_{39}H_{53}KN_4OZr$: C, 64.68; H, 7.38; N, 7.74. Found: C, 64.34; H, 7.67; N, 7.48. ^1H NMR (C_6D_6): δ 0.63−1.29 (m, CH_3, 27 H), 1.90−2.67 (m, CH_2, 18 H), 5.91 (s, pyrrole, 2 H), 6.16 (t, pyrrole, 4 H), 6.96 (q, pyridine, 1 H), 7.24 (d, pyridine, 1 H).

Preparation of 9 and 11. A toluene (50 mL) suspension of **7** (1.80 g, 2.60 mmol) was stirred for 15 h under a CO atmosphere. The resulting light yellow solution was evaporated to dryness. The solid residue was largely soluble in *n*-hexane (50 mL) except for a small amount of solid, which was filtered off. The *n*-hexane solution gave white crystals of **9** (80%) on standing. Anal. Calcd for $C_{39}H_{51}N_4NaOZr$: C, 66.34; H, 7.28; N, 7.94. Found: C, 65.93; H, 7.53; N, 7.79. IR (Nujol): ν(Zr=O) 785 cm^{-1}. ^1H NMR (C_6D_6): δ 0.72−1.24 (m, CH_3, 24 H), 1.96−2.85 (m, CH_2, 16 H), 5.09−5.25 (m, $=CH_2$, 2 H), 5.37 (q, pyrrole, 2 H), 6.11 (t, pyrrole, 2 H), 6.25 (s, pyrrole, 2 H), 7.00 (q, pyridine, 1 H), 7.20 (m, CH, 1 H), 7.32 (d, pyridine, 1 H, J = 8.00 Hz).

9 (1.00 g) in *n*-hexane (50 mL) was hydrolyzed with 20 mL of H_2O. The organic phase was separated, dried over Na_2SO_4, and evaporated to dryness. Following this procedure we obtained white crystals of **11** (70%). Anal. Calcd for $C_{39}H_{54}N_4$: C, 80.92; H, 9.40; N, 9.68. Found: C, 80.45; H, 9.42; N, 9.72. ^1H NMR (CD_2Cl_2): δ 0.38 (t, CH_3, 6 H), 0.57 (t, CH_3, 12 H), 0.70 (t, CH_3, 6 H), 1.65−2.28 (m, CH_2, 16 H), 4.99 (q, $=CH_2$, 1 H), 5.38 (q, $=CH_2$, 1 H), 5.73−6.00 (m, pyrrole, 6 H), 6.22 (s, NH, 1 H), 6.49 (q, $=CH_2$, 1 H), 6.58 (s, NH, 1 H), 7.15 (d, pyridine, 1 H, J = 8.00 Hz), 7.37 (s, NH, 1 H), 7.55 (d, pyridine, 1 H, J = 8.00 Hz).

Preparation of 10. A toluene (200 mL) solution of **8** (3.20 g, 4.40 mmol) was hydrolyzed by addition of 50 mL of H_2O−HCl (5%). The mixture was stirred for 10 min, and then neutralized by K_2CO_3 and stirred for a further 1 h. The organic phase was separated and dried over Na_2SO_4. The solution, when evaporated to dryness, gave a white solid, **10** (61%). Recrystallization from toluene/acetonitrile gave white crystals suitable for X-ray analysis. Anal. Calcd for $C_{39}H_{56}N_4$: C, 80.64; H, 9.72; N, 9.64. Found: C, 80.45; H, 9.81; N, 9.53. ^1H NMR (CD_2Cl_2): δ 0.39 (m, CH_3, 6 H), 0.57 (t, CH_3, 6 H), 0.58 (t, CH_3, 6 H), 0.69 (m, CH_3, 6 H), 0.95 (t, CH_3, 3 H), 1.72 (m, CH_2, 10 H), 2.04 (m, CH_2, 4 H), 2.29 (m, CH_2, 4 H), 5.77 (m, pyrrole, 2 H), 5.86 (q, pyrrole, 2 H), 5.94 (m, pyrrole, 2 H), 6.10 (s, NH, 1 H), 6.50 (s, =NH, 1 H), 7.13 (d, pyridine, 1 H, J = 8.00 Hz), 7.34 (s, NH, 1 H), 7.36 (d, pyridine, 1 H, J = 8.00 Hz).

Preparation of 12. $NbCl_5$ (13.63 g, 50.43 mmol) was added to a toluene (300 mL) solution of $Et_8N_4Li_4(THF)_4$[6c] (43.09 g, 50.50 mmol) at −20 °C, and the reaction mixture was allowed to reach room temperature and was stirred overnight. The mixture was extracted with the mother liquor for 2 h, the solvent was evaporated, and the residue was treated with pentane (200 mL). A brown powder was obtained, which was filtered and dried (74%). Anal. Calcd for $[Et_8N_4NbCl]$, $C_{36}H_{48}ClN_4Nb$: C, 65.03; H, 7.28; N, 8.43. Found: C, 64.99; H, 7.91; N, 8.32. MeLi (21.0 mL, 1.6 M in Et_2O, 33.60 mmol) was added dropwise to a toluene (200 mL) solution of $[Et_8N_4NbCl]$ (22.07 g, 33.17 mmol) at −20 °C, and the reaction mixture was allowed to reach room temperature and was stirred overnight. The resulting green mixture was filtered to eliminate LiCl, the solvent was evaporated to dryness, and the residue was collected with *n*-hexane (120 mL). A green microcrystalline solid was obtained, which was filtered and dried (67%). Anal. Calcd for $C_{37}H_{51}N_4Nb$: C, 68.91; H, 7.98; N, 8.69. Found: C, 69.31; H, 8.23; N, 8.69. ^1H NMR (200 MHz, $C_6D_5CD_3$, room temperature): δ 0.76 (s, CH_3−Nb, 3 H), 0.9−1.1 (m, CH_3, 24 H), 1.9−2.4 (m, CH_2, 16 H), 6.19 (s, CH, 4 H), 6.54 (s, CH, 4 H). ^1H NMR (200 MHz, C_6D_6, room temperature): δ 0.55 (s, CH_3−Nb, 3 H), 0.6−0.8 (m, CH_3, 24 H), 1.6−2.2 (m, CH_2, 16 H), 6.00 (s, CH, 4 H), 6.30 (s, CH, 4 H). ^1H NMR (200 MHz, $C_6D_5CD_3$, 223 K): δ 6.30 (s, CH, 6 H), 6.66 (s, CH, 2 H). ^1H NMR (200 MHz, $C_6D_5CD_3$, 213 K): δ 6.26 (s, CH, 2 H), 6.31 (s, CH, 2 H), 6.34 (s, CH, 2 H), 6.68 (s, CH, 2 H). ^1H NMR (200 MHz, $C_6D_5CD_3$, 203 K): δ 6.24 (s, CH, 2 H), 6.34 (s, CH, 2 H), 6.36 (s, CH, 2 H), 6.70 (s, CH, 2 H).

Preparation of 13. A toluene (125 mL) solution of **12** (5.51 g, 8.54 mmol) was exposed to a CO atmosphere for 1 week. The reaction mixture was concentrated to dryness, and the remaining residue was collected with *n*-hexane (100 mL), yielding yellow crystals suitable for X-ray analysis (81%). Anal. Calcd for $C_{38}H_{51}N_4NbO$: C, 67.84; H, 7.64; N, 8.33. Found: C, 68.07; H, 7.47; N, 8.33. IR: ν(Nb=O) = 908 cm^{-1}, ν(C=N pyridine) = 1547 and 1607 cm^{-1}. ^1H NMR (200 MHz, C_6D_6, room temperature): δ 0.42 (t, CH_3, 6 H, J = 7.1 Hz), 0.7−0.9 (m, CH_3, 18 H), 1.62 (s, CH_3−pyridine, 3 H), 1.8−2.7 (m, CH_2, 16 H), 6.19 (d, CH−pyrrole, 2 H, J = 3.2 Hz), 6.29 (d, CH−pyrrole, 2 H, J = 3.2 Hz), 6.54 (s, CH−pyrrole, 2 H), 6.80 (s, CH−pyridine, 2 H).

Preparation of 14. HCl (16% in H_2O, 50 mL) was added to a toluene (40 mL) solution of **13** (1.5 g, 2.23 mmol). The mixture was vigorously stirred for 8 h, and then it was neutralized with KOH and filtered to eliminate niobium oxide. The aqueous layer was washed with toluene (2 × 50 mL), the toluene solution was dried over Na_2SO_4, and the solvent was evaporated to dryness. A light brown oil was obtained, which crystallized quickly at room temperature (80%) and was recrystallized from hot acetonitrile. Anal. Calcd for $C_{38}H_{54}N_4$: C, 80.51; H, 9.60; N, 9.88. Found: C, 80.03; H, 9.50; N, 9.94. IR: ν(C=N pyridine) 1565 and 1600 cm^{-1}. ν(N−H) 1711 and 3455 cm^{-1}. ^1H NMR (200 MHz, CD_2Cl_2, room temperature): δ 0.60 (q, CH_3, 24 H, J = 7.4 Hz), 1.65−2.2 (m, CH_2, 16 H), 2.30 (s, CH_3−

pyridine, 3 H), 5.8−5.9 (m, CH−pyrrole, 6 H), 6.83 (s, NH, 2 H), 6.99 (s, CH−pyridine, 2 H), 7.21 (s, NH, 1 H).

Preparation of 15. Bu^nLi (142.0 mL, 1.6 M, 227.2 mmol) was added to a THF (150 mL) solution of **5** (42.0 g, 76.0 mmol). The suspension was heated for 1 h at 60 °C and then evaporated to dryness. The oily residue was treated with *n*-hexane (200 mL) to give a white microcrystalline product which was filtered and dried (87%). Anal. Calcd for $C_{45}H_{65}Li_3N_4O_2$: C, 75.61; H, 9.16; N, 7.84. Found: C, 75.66; H, 9.26; N, 7.63. ^1H NMR (C_6D_6): δ 0.51 (m, CH_3, 6 H), 1.17 (m, CH_3 + THF, 26 H), 1.40−2.40 (m, CH_2, 16 H), 3.27 (t, THF, 8 H), 6.14 (d, pyrrole, 2 H, J = 2.80 Hz), 6.34 (s, pyrrole, 2 H), 6.55 (d, pyrrole, 2 H, J = 2.80 Hz), 6.89 (d, pyridine, 2 H, J = 7.80 Hz), 7.16 (t, pyridine, 1 H, J = 7.40 Hz).

Preparation of 16. $HfCl_4{\cdot}THF_2$ (1.80 g, 3.8 mmol) was reacted with a toluene (100 mL) solution of **15** (2.70 g, 3.8 mmol) for 10 h at room temperature. A very insoluble, light-yellow, thick solid formed suddenly, which was isolated and analyzed. Anal. Calcd for $C_{39}H_{49}ClHfN_4{\cdot}3LiCl$: C, 51.20; H, 5.40; N, 6.12. Found: C, 47.83; H, 5.78; N, 5.80.

Preparation of 17. A suspension of complex **16** (3.45 g, 3.77 mmol) was treated with MeLi (2.40 mL, 1.6 M in Et_2O, 3.84 mmol) and heated at 60 °C to dissolve the thick solid. After 5 h, the lithium salts were filtered off, the solution was evaporated to dryness, and the residue was treated with *n*-hexane (50 mL) to yield a light yellow product (75%). Yellow crystals suitable for X-ray analysis were obtained by recrystallization in hexane/toluene. Anal. Calcd for $C_{38}H_{52}HfN_4$: C, 61.40; H, 7.05; N, 7.54. Found: C, 61.61; H, 7.14; N, 7.61. ^1H NMR (C_6D_6): δ -0.32 (s, Me−Hf, 3 H), 0.53 (m, CH_3, 6 H), 0.92 (t, CH_3, 12 H), 1.08 (m, CH_3, 6 H), 1.44−2.56 (m, CH_2, 16 H), 5.75 (m, pyrrole, 2 H), 6.10 (m, pyrrole, 2 H), 6.17 (s, pyrrole, 2 H), 6.67 (d, pyridine, 2 H), 7.05 (t, pyridine, 1 H).

Preparation of 18. A solution of **17** (6.40 g, 8.62 mmol) was exposed to a CO atmosphere for 2−3 days at room temperature. A very insoluble white solid formed, which was filtered and washed with toluene (42%). Anal. Calcd for $C_{39}H_{52}HfN_4O$: C, 60.73; H, 6.79; N, 7.26. Found: C, 60.15; H, 7.06; N, 7.06. IR: ν(Hf=O), 826 cm^{-1}.

Preparation of 19. A THF (350 mL) solution of **17** (19.5 g, 26.0 mmol) was stirred under a CO atmosphere for 4−5 days. The THF was removed, and the residue was hydrolyzed with a mixture of toluene/H_2O (200/50 mL). The organic phase was layered and dried. The mixture was concentrated to dryness to give an oil which crystallized as a white solid. This solid was stirred in acetonitrile, filtered, quickly washed with acetonitrile, and dried. A beige-white product was obtained (68%), and white crystals suitable for X-ray analysis were obtained by recrystallization from acetonitrile. Anal. Calcd for $C_{39}H_{54}N_4$: C, 80.92; H, 9.40; N, 9.68. Found: C, 80.81; H, 9.46; N, 9.59. ^1H NMR (CD_2Cl_2): δ 0.42 (t, CH_3, 6 H), 0.53 (t, CH_3, 6 H), 0.60 (t, CH_3, 12 H), 1.51−2.37 (m, CH_2, 16 H), 1.92 (s, CH_3−pyridine, 3 H), 5.70 (t, pyrrole, 1 H), 5.75 (m, pyrrole, 2 H), 5.86 (t, pyrrole, 1 H), 6.19 (s, NH, 1 H), 7.00 (q, J = 7.80 Hz, pyridine, 2 H), 7.22 (m, J = 6.40 Hz, CH_3−pyridine, 2 H), 7.32 (s, NH, 1 H), 7.54 (t, J = 7.80 Hz, pyridine, 1 H).

X-ray Crystallography. The crystals of compounds **8, 13, 17,** and **19** selected for study were mounted in glass capillaries and sealed under nitrogen. The reduced cells were obtained with the use of TRACER.[20] Crystal data and details associated with structure refinement are given in Tables 1 and S1. Data were collected at room temperature (295 K) on a single-crystal diffractometer. For intensities and background, individual reflection profiles were analyzed.[21] The structure amplitudes were obtained after the usual Lorentz and polarization corrections[22] and the absolute scale was established by the Wilson method.[23] The crystal quality was tested by ψ scans showing that crystal absorption effects could be neglected for compound **19.** Data were corrected for absorption using the program ABSORB[24] for complexes **8** and **19** and a semiempirical method[25] for complexes **13** and **17.** The function minimized during the full-matrix least-squares refinement was $\sum w|\Delta F^2|$ for complexes **8, 17,** and **19.** For complex **13** the function minimized was $\sum w(\Delta F^2)^2$. Weights were applied according to the scheme $\{w = k/[\sigma^2(F_o) + g|F_o|^2]\}$ for complexes **8, 17,** and **19,** and $w = 1/[\sigma^2(F_o^2) + (gP)^2]$ with $P = (F_o^2 + 2F_c^2)/3$ for complex **13.** Anomalous scattering corrections were included in all structure factor calculations.[26b] Scattering factors for neutral atoms were taken from ref 26a for non-hydrogen atoms and from ref 27 for hydrogen atoms. Among the low-angle reflections, no correction for secondary extinction was deemed necessary.

Solution and refinement were based on the observed reflections for complexes **8, 17,** and **19** and on the unique total data for complex **13.** The structures were solved by the heavy-atom method starting from a three-dimensional Patterson map for complexes **8** and **17.** For **13** and **19,** the structure was solved using SHELX86.[28] Refinement was first done isotropically and then anisotropically for non-H atoms, excluding those affected by disorder. The structures of complexes **17** and **19** were refined straightforwardly. In complex **8** the C31 methyl carbon of molecule B was affected by disorder and isotropically refined over two positions (unprimed and primed) with the site occupation factors given in Table S2. In complex **13,** the *n*-hexane solvent molecule of crystallization was isotropically refined with a site occupation factor of 0.5.

For compounds **8, 17,** and **19** the hydrogen atoms were located from difference Fourier maps. For compound **13** they were put in geometrically calculated positions. They were introduced in the subsequent refinements as fixed atom contributions with isotropic Us fixed at 0.08 Å^2 for complex **17,** 0.10 Å^2 for **8** and **13,** and 0.12 Å^2 for **19.** Hydrogen atoms related to the disordered C30−C31 ethyl chain of molecule B in complex **8** and to the *n*-hexane solvent molecule in complex **13** were ignored.

The final difference map showed no unusual features, with no significant peak above the general background. Final atomic coordinates are listed in Tables S2−S5 for non-H atoms and in Tables S6−S9 for hydrogens. Thermal parameters are given in Tables S10−S13, bond distances and angles in Tables S14−S17.[29]

Acknowledgment. We would like to thank the "Fonds National Suisse de la Recherche Scientifique" (Grant No. 20-33420-92) and Ciba-Geigy S.A. (Basel) for financial support.

Supplementary Material Available: Tables giving crystal data and details of the structure determination, bond lengths, bond angles, anisotropic thermal parameters, and hydrogen atom locations (27 pages); observed and calculated structure factor tables (56 pages). This material is contained in many libraries on microfiche, immediately follows this article in the microfilm version of the journal, can be ordered from the ACS, and can be downloaded from the Internet; see any current masthead page for ordering information and Internet access instructions.

JA9433030

(20) Lawton, S. L.; Jacobson, R. A. TRACER (a cell reduction program); Ames Laboratory; Iowa State University of Science and Technology: Ames, IA, 1965.

(21) Lehmann, M .S.; Larsen, F. K. *Acta Crystallogr., Sect. A: Cryst. Phys., Diffr., Theor. Gen. Crystallogr.* **1974,** *A30,* 580−584.

(22) Data reduction, structure solution, and refinement were carried out on an IBM AT personal computer equipped with an INMOS T800 transputer and on an ENCORE 91 computer using the following: Sheldrick, G. SHELX-76. System of Crystallographic Computer Programs; University of Cambridge: Cambridge, U.K., 1976.

(23) Wilson, A. J. C. *Nature* **1942,** *150,* 151.

(24) ABSORB, a Program for F_o Absorption Correction. Ugozzoli, F. *Comput. Chem.* **1987,** *11,* 109.

(25) North, A. C. T.; Phillips, D. C.; Mathews, F. S. *Acta Crystallogr., Sect. A: Cryst. Phys., Diffr., Theor. Gen. Crystallogr.* **1968,** *A24,* 351.

(26) (a) *International Tables for X-ray Crystallography*; Kynoch Press: Birmingham, England, 1974; Vol. IV, p 99; (b) p 149.

(27) Stewart, R. F.; Davidson, E. R.; Simpson, W. T. *J. Chem. Phys.* **1965,** *42,* 3175.

(28) Sheldrick, G. SHELX-86: Program of the Solution of Crystal Structures; University of Göttingen, Germany, 1986.

(29) See paragraph at the end regarding supplementary material.